

University of Wollongong

## Research Online

---

Faculty of Science, Medicine and Health -  
Papers: Part B

Faculty of Science, Medicine and Health

---

1-1-2019

### High temperature expulsion of thermolabile groups for pore-space expansion in metal-organic frameworks

Macguire Bryant

*University of Wollongong, mrb940@uowmail.edu.au*

Timothy Ablott

*University of Wollongong, taa600@uowmail.edu.au*

Shane Telfer

*Massey University*

Lujia Liu

*Northwestern University*

Christopher Richardson

*University of Wollongong, crichard@uow.edu.au*

Follow this and additional works at: <https://ro.uow.edu.au/smhpapers1>

---

#### Publication Details Citation

Bryant, M., Ablott, T., Telfer, S., Liu, L., & Richardson, C. (2019). High temperature expulsion of thermolabile groups for pore-space expansion in metal-organic frameworks. Faculty of Science, Medicine and Health - Papers: Part B. Retrieved from <https://ro.uow.edu.au/smhpapers1/488>

Research Online is the open access institutional repository for the University of Wollongong. For further information contact the UOW Library: [research-pubs@uow.edu.au](mailto:research-pubs@uow.edu.au)

---

## High temperature expulsion of thermolabile groups for pore-space expansion in metal-organic frameworks

### Abstract

Direct radiative heating at 200 °C quantitatively converts sulfoxide-tags to desirable vinyl groups on a porous zinc(ii) metal-organic framework analogue of IRMOF-9. The transformation results in an expansion of the pore volume of the framework and a higher surface area. The framework topology and crystallinity are preserved during thermolysis, as established by powder X-ray diffraction, thermal analysis and computational studies. Importantly, the volatile by-product is chemically benign and escapes without damaging the framework. In this way, the post-synthetic thermolysis yields a material with identical properties to that prepared by direct synthesis. This work expands the repertoire of post-synthetic thermochemistry for MOFs and demonstrates that high-temperature processes can be compatible with the retention of important framework properties.

### Publication Details

Bryant, M. R., Ablott, T. A., Telfer, S. G., Liu, L. & Richardson, C. (2019). High temperature expulsion of thermolabile groups for pore-space expansion in metal-organic frameworks. *CrystEngComm*, 21 (1), 60-64.

## ARTICLE

# High temperature expulsion of thermolabile groups for pore-space expansion in metal-organic frameworks

Cite this: DOI: 10.1039/x0xx00000x

Received 00th January 2012,  
Accepted 00th January 2012

DOI: 10.1039/x0xx00000x

[www.rsc.org/](http://www.rsc.org/)

Macguire R. Bryant,<sup>a</sup> Timothy A. Ablott,<sup>a</sup> Shane G. Telfer,<sup>b</sup> Lujia Liu,<sup>c</sup> and Christopher Richardson<sup>\*a</sup>

Direct radiative heating at 200 °C quantitatively converts sulfoxide-tags to desirable vinyl groups on a porous zinc(II) metal-organic framework analogue of IRMOF-9. The transformation results in an expansion of the pore volume of the framework and a higher surface area. The framework topology and crystallinity are preserved during thermolysis, as established by powder X-ray diffraction, thermal analysis and computational studies. Importantly, the volatile by-product is chemically benign and escapes without damaging the framework. In this way, the post-synthetic thermolysis yields a material with identical properties to that prepared by direct synthesis. This work expands the repertoire of post-synthetic thermochemistry for MOFs and demonstrates that high-temperature processes can be compatible with the retention of important framework properties.

## Introduction

The concept of tailored molecular building blocks self-assembling in a single step to produce functional porous crystalline materials, such as metal-organic frameworks (MOFs), is immeasurably attractive. A much-vaunted asset in the assembly of MOFs is the chemical mutability of their building blocks. However, direct substitution of building blocks is not always compatible with isorecticular synthesis, that is, when a specific framework topology is targeted. MOF post-synthetic modification (PSM) is a deliberate strategy to modify the framework after its assembly and can overcome problems of chemical incompatibility. Amongst the many variants of MOF PSM, functionalisation of the bridging ligands while maintaining framework topology is enduring.

We are involved in a programme of thermally-promoted post-synthetic modification of MOFs.<sup>1-4</sup> Provided that the requisite chemical functionality can be incorporated in the framework, thermally-promoted modifications are straightforward to implement as they simply require heating. Most modifications are eliminations and include thermolysis of *tert*-butoxycarbamates,<sup>5-7</sup> hemiaminals,<sup>8</sup> carboxylic acids,<sup>9</sup> and azides.<sup>10-12</sup> Recently, this concept has been extended to deliberate defect introduction by full thermolytic bridging linker removal under oxidising conditions.<sup>13, 14</sup> From these examples it is evident that post-synthetic elimination chemistry concurrent delivers new

chemical functionality and increases pore size by cleaving groups or bridging ligands from the framework.

We considered vinyl tag groups to be an important post-synthetic target given their potential interactions with guest molecules and scope for further derivatisation. Such groups can be incorporated *via* direct synthesis under mild conditions<sup>15, 16</sup> but are prone to polymerisation at elevated temperatures in the presence of strong Lewis and Bronsted acids, potentially precluding many MOF synthesis conditions. Thus, a post-synthetic pathway to vinyl groups represents a worthwhile addition to the growing library of thermally-promoted modifications. Sun *et al.* post-synthetically generated vinyl groups from a hydroxyethyl-functionalised MOF by elimination of water at 250 °C, in what appears to be a Lewis acid induced process by adjacent Zn SBUs; unfortunately, complete loss of framework crystallinity and porosity accompanied the elimination.<sup>17</sup> Therefore, we sought to extend our work on thermally-promoted post-synthetic elimination chemistry of alkyl sulfoxides<sup>3</sup> to the generation of vinyl tags and report the results here. We show the modification proceeds quantitatively under direct radiative heating in a solventless process with no framework damage, as demonstrated by comparison to material prepared from direct synthesis (Fig. 1).

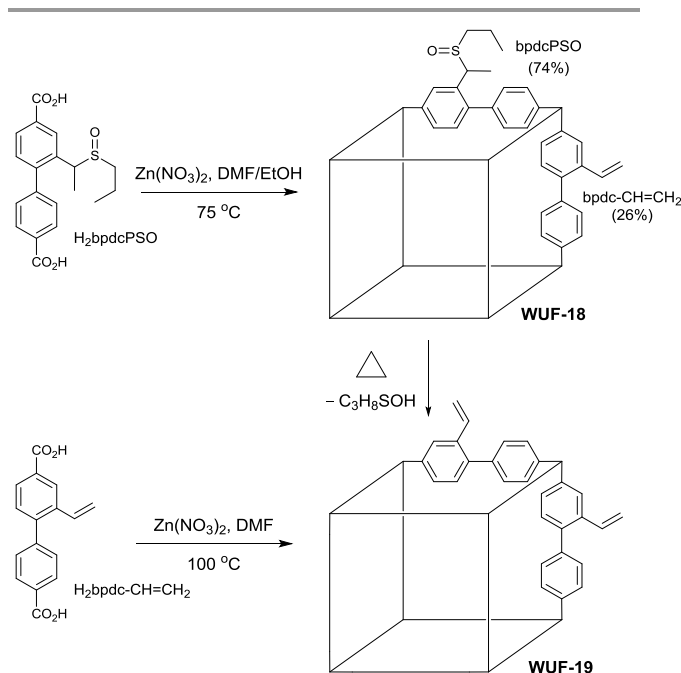


**Fig. 1** The structures of  $H_2bpdCPSO$  and  $H_2bpdC-CH=CH_2$  and the synthetic conditions to form WUF-18 and WUF-19.

## Experimental

All chemicals used were of analytical grade and purchased from either Sigma Aldrich, VWR Australia or Ajax Finechem Pty Ltd. The synthetic procedures for  $H_2bpdCPSO$  and  $H_2bpdC-CH=CH_2$  are provided in the ESI.  $^1H$  NMR and  $^{13}C$  NMR spectra were obtained using a Bruker NMR spectrometer operating at 400 MHz for  $^1H$  and 101 MHz for  $^{13}C$ .  $^1H$  NMR spectra were referenced to the residual proton peaks at 2.50 ppm ( $d_6$ -DMSO) or 7.27 ppm ( $CDCl_3$ ).  $^{13}C$  NMR spectra were referenced to the solvent peaks at 39.6 ppm ( $d_6$ -DMSO) or 77.7 ppm ( $CDCl_3$ ). For  $^1H$  NMR analysis, MOF samples (~5 mg) were digested by adding 35% DCl in  $D_2O$  (2  $\mu L$ ) and DMSO (500  $\mu L$ ) and waiting until a solution was obtained.

Simultaneous thermogravimetric and differential scanning calorimetry (TG-DSC) data were recorded using a Netzsch STA449F3 at 10  $^{\circ}C/min$  under  $N_2$  flow at 20  $cm^3/min$  for WUF-18 and WUF-19PSM, and 10  $^{\circ}C/min$  under 5%  $O_2$  in  $N_2$  at 40  $cm^3/min$  for WUF-19.

Powder X-ray diffraction (PXRD) patterns were recorded on a GBC-MMA X-ray diffractometer with samples mounted on 1"  $SiO_2$  substrates. Experimental settings in the  $2\theta$  angle range of 3–30 $^{\circ}$  with 0.02 $^{\circ}$  step size and 1 $^{\circ} min^{-1}$  scan speed were used for as-synthesised WUF-18 and WUF-19 and 0.04 $^{\circ}$  step size with 3 $^{\circ} min^{-1}$  scan speed for activated WUF-18 and WUF-19(PSM).

Single crystal diffraction data were collected using a Rigaku Spider diffractometer equipped with a MicroMax MM007 rotating anode generator (Cu  $K\alpha$  radiation,  $\lambda = 1.54180$   $\text{\AA}$ ), high-flux Osmic multilayer mirror optics, and a curved image-plate detector at 292 K. The data were

integrated and scaled and averaged with FS Process.<sup>18</sup> The crystal structures were solved by direct methods using SHELXS-97 and refined against  $F^2$  on all data by full-matrix least-squares with SHELXL-97.<sup>19</sup>

Gas adsorption studies were carried out using a Quantachrome Autosorb MP instrument and high purity nitrogen (99.999%) gas. Surface areas were determined using Brunauer-Emmett-Teller (BET) calculations. Freeze drying was carried out in a Christ Alpha 1-2 LDplus Freeze Dryer. Elemental microanalysis was performed by the Chemical Analysis Facility, Macquarie University, Australia.

### Synthetic procedure for WUF-18

A solution of  $H_2bpdCPSO$  (10.3 mg, 0.029 mmol) and  $Zn(NO_3)_2 \cdot 6H_2O$  (11.6 mg, 0.040 mmol) dissolved in 3:1 DMF:EtOH (1.3  $cm^3$ ) was placed in an oven pre-heated to 75  $^{\circ}C$  for 48 hours to produce colourless, cubic-shaped crystals. The DMF solution was exchanged five times with fresh DMF at room temperature over three days, then with  $CH_2Cl_2$  over three days, and then with benzene over three days. The sample was freeze dried for one hour, before being heated at 120  $^{\circ}C$  for five hours under vacuum to produce an activated sample. Yield 9.1 mg (73%). Found: C, 49.38%; H, 3.96%; N, 0%; S, 5.03%, Calc. for  $[Zn_4O(C_{19}H_{18}O_5S)_{2.22}(C_{16}H_{10}O_4)_{0.78}] \cdot 2H_2O$ : C: 49.84%; H: 3.96%; N: 0%; S: 5.39%.

### Synthetic procedure for WUF-19PSM

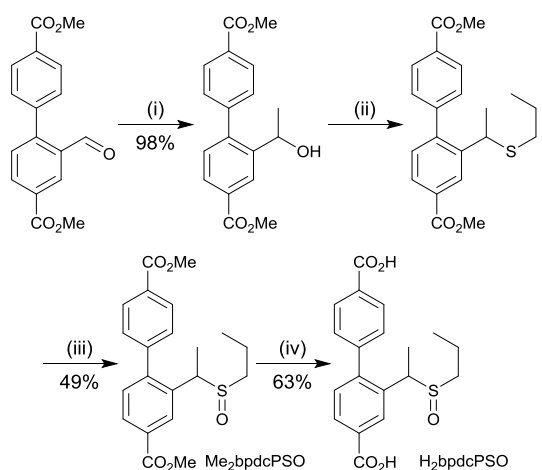
Samples were produced by heating WUF-18 at 10  $^{\circ}C min^{-1}$  under  $N_2$  at 20  $cm^3 min^{-1}$  to 205  $^{\circ}C$  and holding for 60 minutes in a TG-DSC analyser.

### Synthetic procedure for WUF-19

A solution of  $H_2bpdC-CH=CH_2$  (29.8 mg, 0.111 mmol) and  $Zn(NO_3)_2 \cdot 6H_2O$  (44.3 mg, 0.148 mmol) dissolved in DMF (2.25  $cm^3$ ) was placed in an oven pre-heated to 100  $^{\circ}C$  for 24 hours to produce yellow-coloured crystals. The DMF solution was exchanged three times for fresh DMF at 100  $^{\circ}C$ , then at room temperature for  $CH_2Cl_2$  over two days, and then for benzene over two days. The sample was freeze dried for one hour, and then heated at 120  $^{\circ}C$  for five hours under vacuum to produce an activated sample. Yield 16.8 mg (42%).

## Results and discussion

$H_2bpdCPSO$  was synthesised in four steps starting from dimethyl 2-formyl-[1,1'-biphenyl]-4,4'-dicarboxylate *via* a Grignard reaction with methylmagnesium bromide,  $ZnI_2$ -catalysed thiolation, oxidation with mCPBA and hydrolysis in aqueous base (Scheme 1). The compound was characterised by  $^1H$  and  $^{13}C$  NMR spectroscopy.



**Scheme 1:** Synthetic pathway to  $H_2bpdC-PSO$ ; (i)  $MeMgBr$ , THF, 0 °C; (ii) Propane thiol,  $ZnI_2$ , DCE, reflux; (iii)  $mCPBA$ ,  $CH_2Cl_2$ , 0 °C; (iv) 1M NaOH, MeOH/THF, rt.

There are two possible *syn*-eliminations of the sulfoxide tags, as shown in Fig. 2. Path A is favoured, affording a vinyl group and releasing 1-propanesulfenic acid. This conversion is facile in solution and temperature control was important to limit conversion to the vinyl group during ligand synthesis.

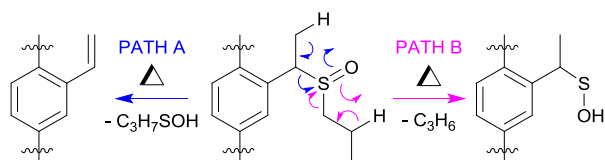


**Fig. 2** Possible *syn*-elimination pathways of the sulfoxide tag groups.

For this reason, we applied typical solvothermal conditions for zinc IRMOF formation to  $Me_2bpdC-PSO$  in order to find conditions that minimised conversion of the sulfoxide groups to vinyl groups (Table S1). The best results were obtained at 75 °C in 3:1 DMF:EtOH where only 10% conversion was found after 24 hours. The reaction of  $H_2bpdC-PSO$  and  $Zn(NO_3)_2 \cdot 6H_2O$  required, however, 48 hours at 75 °C in 3:1 DMF:EtOH solution to produce colourless, blocky crystals of WUF-18. Analysis by  $^1H$  NMR spectroscopy of these crystals digested in  $DCI/d_6-DMSO$  revealed 26% of linkers were  $bpdC-CH=CH_2$  (Fig. S9), which is attributable to the longer reaction time. Elemental analysis on activated WUF-18 was consistent with the  $^1H$  NMR data in fitting the molecular formula  $Zn_4O(bpdC-PSO)_{2.22}(bpdC-CH=CH_2)_{0.78} \cdot 2H_2O$ .

As a basis for comparison in our post-synthetic studies, we prepared  $Zn_4O(bpdC-CH=CH_2)_3$  (WUF-19) as yellow crystals via a direct synthesis starting from  $H_2bpdC-CH=CH_2$  (Fig. 1). Analysis by single crystal X-ray diffraction showed WUF-19 crystallises in the space group  $C2/m$  as a pair of interpenetrating **pcu** networks (Fig. 3). We have found this to be a common space group for a functionalised IRMOF-9-type compounds.<sup>1, 4, 20-22</sup> A full

description of the asymmetric unit of this structure can be found in the ESI. At their closest point, the frameworks are only 3.5 Å apart but reticulate into a structure with pore sizes of ~5 and ~10 Å (Fig. 3). Similar bimodal pore features have been identified for IRMOF-9-type systems.<sup>23</sup> The smaller pore is bounded by  $Zn_4O$  SBUs and entraps a solvate water molecule, while the larger pore system runs parallel to the crystallographic *c*-axis (Fig. 3b). The vinyl tag groups were not located on Fourier maps, most likely due to positional and rotational disorder, and therefore were implanted in chemically sensible positions to complete the crystallographic model.  $^1H$  NMR spectroscopy of digested WUF-19 crystals showed the vinyl groups were incorporated unaltered into the framework.

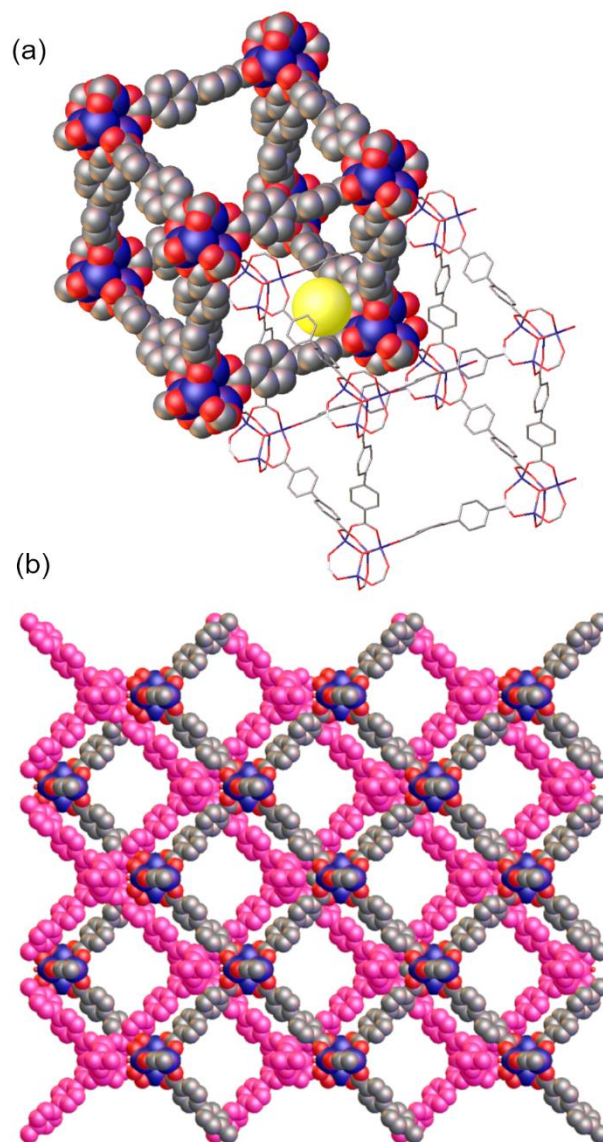


**Fig. 3a** A perspective view of the small pore in the interpenetrating networks of WUF-19, b) A view of the larger channels that run parallel to the crystallographic *c*-axis. Vinyl tag groups and hydrogen atoms are not shown to aid clarity.

The matching PXRD patterns of WUF-18 and WUF-19 with the pattern calculated from the SCXRD analysis (Fig. 4) establishes that bulk samples of these compounds are isorecticular, as expected, and phase pure.

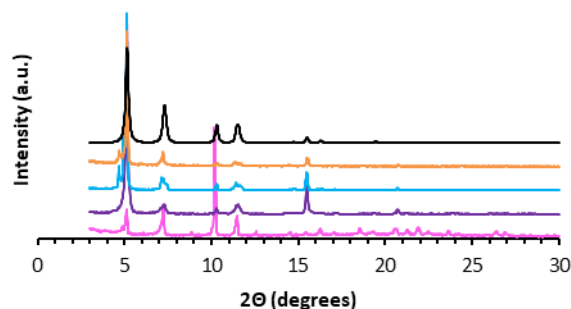


**Fig. 4** PXRD patterns for 'as-synthesised' WUF-18 (magenta), activated WUF-19PSM (purple), 'as-synthesised' WUF-19 (blue), activated WUF-19 (orange) and the calculated pattern of WUF-19 (black).

### Thermally-promoted post-synthetic chemistry

We used TGA to follow the thermally-promoted post-synthetic chemistry of WUF-18 (Fig. 1). Fig. 5 shows the thermogravimetrogram of activated WUF-18, recorded under a flowing atmosphere of  $N_2$ . Following a mass loss consistent with desorption of a small amount of surface water (2.0% at 100 °C), there is a loss of 13.6% from 150–350 °C, which is approximately that expected for the elimination of 1-propanesulfenic acid (16.0%). The mass loss observed above 400 °C is due to framework decomposition. In comparison, activated WUF-19 recorded under a flowing atmosphere of 5%  $O_2$  in  $N_2$  does not show any mass loss until rapid decomposition around 400 °C.

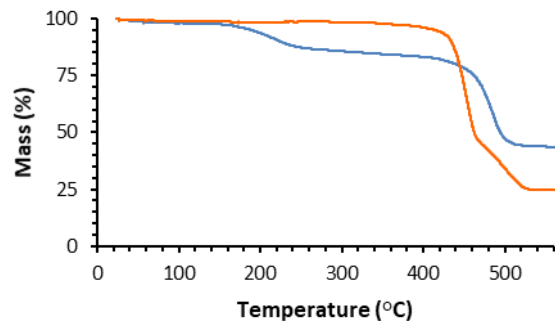


**Fig. 5** TGA curves for activated WUF-18 (blue) and WUF-19 (orange).

WUF-19PSM was prepared by heating WUF-18 to 205 °C for one hour under  $N_2$ . Analysis by  $^1H$  NMR spectroscopy after digestion in  $DCI/d_6$ -DMSO confirmed the quantitative nature of the elimination, as the spectrum showed WUF-19PSM was composed solely of bpdC- $CH=CH_2$  linkers (Fig. S9). In addition, WUF-19PSM

retains full crystallinity in comparison to the theoretical and experimental PXRD patterns of WUF-18 and WUF-19 (Fig. 4). The excellent maintenance of crystallinity demonstrates that expulsion of 1-propanesulfenic acid does not damage the lattice, despite the high temperature.

### Gas adsorption studies

In our experience, gas adsorption isotherms are a more sensitive measure of framework integrity after post-synthetic modifications than PXRD.<sup>1-4</sup> With this in mind, we recorded  $N_2$  isotherms at 77 K for WUF-18, WUF-19 and WUF-19PSM to ascertain the effects of the modification on surface areas and pore volumes. Fig. 6 shows the adsorption isotherms (see Fig. S14-16 for full adsorption-desorption isotherms) and the surface areas and pore volumes of the frameworks are summarised in Table 1. Each isotherm displays Type I behaviour typical of microporous MOFs. Significant increases in surface area of over 300  $m^2/g$  and in pore volume of  $\sim 0.11$   $cm^3/g$  are observed moving from WUF18 to the post-modified MOF, WUF-19PSM. This is expected given the elimination of 1-propanesulfenic acid results in smaller sized vinyl groups attached to the framework. Increases in surface area and pore volume are commonly observed when groups were cleaved from MOFs.<sup>3, 12, 24, 25</sup> It is also significant that the isotherms, apparent surface areas and pore volumes for WUF-19PSM are virtually identical to WUF-19 prepared by direct synthesis and compare favourably to the geometric surface area calculation of 2070  $m^2/g$  calculated using a rolling nitrogen simulation method (see ESI for details). This demonstrates that this PSM delivers materials directly comparable to direct synthesis and reinforces the gentle nature of this solventless thermal modification.

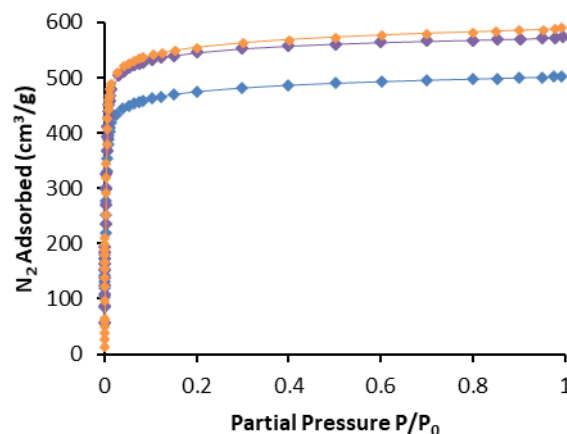


**Fig. 6** Nitrogen gas adsorption isotherms at 77 K for WUF-18 (blue), WUF-19PSM (purple) and WUF-19 (orange).

Table 1. Apparent surface areas and pore volumes.

	SA (m <sup>2</sup> g <sup>-1</sup> ) <sup>a</sup>	Pore Volume (cm <sup>3</sup> g <sup>-1</sup> ) <sup>b</sup>
WUF-18	1891	0.78
WUF-19PSM	2200	0.89
WUF-19	2228	0.86

<sup>a</sup> Apparent surface area from BET analysis for N<sub>2</sub> adsorbate at 77 K <sup>b</sup> At P/P<sub>0</sub> 0.99.

## Conclusions

In summary, a new, high-temperature, thermally-promoted reaction for MOFs is reported here. This example expands the small but growing library of thermolytic post-synthetic modifications that increase pore volumes and raise surface areas of MOFs. The simple, gentle and reagentless nature of this approach highlights the benefits of post-synthetic thermolysis.

## Acknowledgements

MRB and TAA acknowledge the Australian Government for Australian Government Research Training Program Awards. CR thanks the University of Wollongong for financial support.

## Notes and references

<sup>a</sup> School of Chemistry and Biomolecular Science, University of Wollongong, Wollongong NSW 2522, Australia; Fax: +61 2 4221 4287; Tel: +61 2 4221 3254; E-mail: [chris\\_richardson@uow.edu.au](mailto:chris_richardson@uow.edu.au)

<sup>b</sup> MacDiarmid Institute of Advanced Materials and Nanotechnology, Institute of Fundamental Sciences, Massey University, Palmerston North 4442, New Zealand

<sup>c</sup> Department of Chemistry, Northwestern University, 2145 Sheridan Road, Evanston, Illinois 60208-3113, United States

Electronic Supplementary Information (ESI) available: synthetic procedures, <sup>1</sup>H and <sup>13</sup>C NMR spectra for H<sub>2</sub>bpcPSO and H<sub>2</sub>bpc-CH=CH<sub>2</sub>, <sup>1</sup>H NMR digestion spectra for WUF-18 and WUF-19PSM, additional TG-DSC data, PXRD data, gas adsorption isotherms and surface area calculations. CCDC 1872644.

1. A. D. Burrows, S. O. Hunter, M. F. Mahon and C. Richardson, *Chem. Commun.*, 2013, **49**, 990-992.
2. L. Tshering, S. O. Hunter, A. Nikolich, E. Minato, C. M. Fitchett, D. M. D'Alessandro and C. Richardson, *CrystEngComm*, 2014, **16**, 9158-9162.
3. M. R. Bryant and C. Richardson, *CrystEngComm*, 2015, **17**, 8858-8863.
4. T. A. Ablott, M. Turzer, S. G. Telfer and C. Richardson, *Cryst. Growth Des.*, 2016, **16**, 7067-7073.
5. R. K. Deshpande, J. L. Minnaar and S. G. Telfer, *Angew. Chemie Int. Ed.*, 2010, **49**, 4598-4602.
6. A. Sen Gupta, R. K. Deshpande, L. Liu, G. I. N. Waterhouse and S. G. Telfer, *CrystEngComm*, 2012, **14**, 5701.
7. D. J. Lun, G. I. N. Waterhouse and S. G. Telfer, *J. Am. Chem. Soc.*, 2011, **133**, 5806-5809.
8. W. Morris, C. J. Doonan and O. M. Yaghi, *Inorg. Chem.*, 2011, **50**, 6853-6855.

9. N. Reimer, B. Gil, B. Marszalek and N. Stock, *CrystEngComm*, 2012, **14**, 4119-4125.
10. J. G. Vitillo, T. Lescouet, M. Savonnet, D. Farrusseng and S. Bordiga, *Dalton Trans.*, 2012, **41**, 14236-14238.
11. T. Lescouet, J. G. Vitillo, S. Bordiga, J. Canivet and D. Farrusseng, *Dalton Trans.*, 2013, **42**, 8249-8258.
12. S. Ganguly, P. Pachfule, S. Bala, A. Goswami, S. Bhattacharya and R. Mondal, *Inorg. Chem.*, 2013, **52**, 3588-3590.
13. B. Bueken, N. Van Velthoven, A. Krajnc, S. Smolders, F. Taulelle, C. Mellot-Draznieks, G. Mali, T. D. Bennett and D. De Vos, *Chem. Mater.*, 2017, **29**, 10478-10486.
14. L. Feng, S. Yuan, L. L. Zhang, K. Tan, J. L. Li, A. Kirchon, L. M. Liu, P. Zhang, Y. Han, Y. J. Chabal and H. C. Zhou, *J. Am. Chem. Soc.*, 2018, **140**, 2363-2372.
15. G. Distefano, H. Suzuki, M. Tsujimoto, S. Isoda, S. Bracco, A. Comotti, P. Sozzani, T. Uemura and S. Kitagawa, *Nat. Chem.*, 2013, **5**, 335.
16. C. Satheeshkumar, H. J. Yu, H. Park, M. Kim, J. S. Lee and M. Seo, *J. Mater. Chem. A*, 2018, DOI: 10.1039/C8TA03803A.
17. F. Sun, Z. Yin, Q. Q. Wang, D. Sun, M. H. Zeng and M. Kurmoo, *Angew. Chem. Int. Ed.*, 2013, **52**, 4538-4543.
18. *Rigaku Corporation: Tokyo, Japan, 1996.*
19. G. M. Sheldrick, *Acta Cryst. A*, 2008, **64**, 112-122.
20. A. D. Burrows, C. Frost, M. F. Mahon and C. Richardson, *Angew. Chem. Int. Ed.*, 2008, **47**, 8482-8486.
21. A. D. Burrows, C. G. Frost, M. F. Mahon and C. Richardson, *Chem. Commun.*, 2009, DOI: 10.1039/b906170c, 4218-4220.
22. M. R. Bryant, A. D. Burrows, C. J. Kepert, P. D. Southon, O. T. Qazvini, S. G. Telfer and C. Richardson, *Cryst. Growth Des.*, 2017, **17**, 2016-2023.
23. R. Babarao, C. J. Coghlan, D. Rankine, W. M. Bloch, G. K. Gransbury, H. Sato, S. Kitagawa, C. J. Sumbly, M. R. Hill and C. J. Doonan, *Chem. Commun.*, 2014, **50**, 3238-3241.
24. T. Gadzikwa, O. K. Farha, C. D. Malliakas, M. G. Kanatzidis, J. T. Hupp and S. T. Nguyen, *J. Am. Chem. Soc.*, 2009, **131**, 13613-13615.
25. K. K. Tanabe, C. A. Allen and S. M. Cohen, *Angew. Chem. Int. Ed.*, 2010, **49**, 9730-9733.